

Mcl1p Is a Polymerase α Replication Accessory Factor Important for S-Phase DNA Damage Survival

Dewight R. Williams* and J. R. McIntosh

Department of Molecular, Cellular, and Developmental Biology, University of Colorado, Boulder, Colorado

Received 15 June 2004/Accepted 26 October 2004

Mcl1p is an essential fission yeast chromatin-binding protein that belongs to a family of highly conserved eukaryotic proteins important for sister chromatid cohesion. The essential function is believed to result from its role as a Pol1p (polymerase α) accessory protein, a conclusion based primarily on analogy to Ctf4p's interaction with Pol1p. In this study, we show that Mcl1p also binds to Pol1p with high affinity for the N terminus of Pol1p during S phase and DNA damage. Characterization of an inducible allele of *mcl1*⁺, *nmt41 mcl1-MH*, shows that altered expression levels of Mcl1p lead to sensitivity to DNA-damaging agents and synthetic lethality with the replication checkpoint mutations *rad3* Δ , *rqh1* Δ , and *hsk1-1312*. Further, we find that the overexpression of the S-phase checkpoint kinase, Cds1, or the loss of Hsk1 kinase activity can disrupt Mcl1p's interaction with chromatin and Pol1p during replication arrest with hydroxyurea. We take these data to mean that Mcl1p is a dynamic component of the polymerase α complex during replication and is important for the replication stress response in fission yeast.

Pol1 is the largest subunit of the heterotetrameric polymerase α holoenzyme (pol-prim), where it serves as the deoxyribonucleotidyl transferase (5, 39). pol-prim is essential for DNA replication initiation because it synthesizes the nascent DNA on a single-strand DNA template (57). Due to the inherent 5' to 3' directionality of DNA synthesis, it is required to initiate the discontinuous synthesis of DNA on the lagging strand every 100 to 300 bp (63). The synthesis of the short, initiator primer by pol-prim establishes the S-phase checkpoint in fission yeast and *Xenopus* (15, 37, 68). This conserved signal transduction pathway ensures that S phase is complete prior to chromosome segregation (23). In addition, pol-prim function is important for telomere length regulation, DNA recombination, and site-specific heterochromatin formation (1, 3, 9, 11, 17, 20, 36, 41, 51, 52, 66).

Mcl1p and Ctf4p are yeast members of a eukaryotic family of WD (tryptophan and aspartic acid) repeat proteins that are important for genome stability. This important function is believed to result from a regulatory role for Pol1p. The strongest support for this conclusion comes from Ctf4p's being the principal budding yeast protein that bound to a Pol1p affinity column (38). All fungal mutants of this protein family are dependent on components of the S-phase checkpoint for survival, and they show strong genetic interactions with replication factors important for lagging strand synthesis, such as *dna2* helicase and *fen1* nuclease (20, 22, 32, 66). Characterizations of these mutants have revealed chromosome loss resulting from both decreased sister chromatid cohesion, which promotes missegregation of chromosomes during mitosis, and decreased fidelity of DNA replication, which promotes mitotic chromosomal rearrangements (21, 32, 38, 58, 66). In *Schizosaccharomyces pombe*, both of these mechanisms for chromosome loss can be attributed to Pol1p function, since Pol1 mu-

tants have both sister chromatid cohesion defects and replication defects (1, 3, 41). Additional support for the idea that Ctf4p and Mcl1p regulate Pol1p during replication comes from their effect on telomere length homeostasis, which has a distinct Pol1p-dependent component.

CTF4 and *mcl1* mutants are exquisitely sensitive to the DNA-methylating agent methyl methanesulfonate (MMS). Detection of DNA alkylation occurs primarily during DNA replication and results in slower DNA replication, which occurs due to the S-phase checkpoint and through modified bases forming a blockade to replication (48). The checkpoint responses in *S. pombe* and *Saccharomyces cerevisiae* are completely dependent on the checkpoint kinases Rad3 (*S. pombe*) and Mec1 (*S. cerevisiae*) and their downstream effectors Cds1 (*S. pombe*) and Rad53 (*S. cerevisiae*). Their activation inhibits DNA replication initiation from "late" initiating origins (35, 53), and both act to maintain ongoing replication forks that stall at sites of DNA damage (45, 56, 61, 62). Recent work on two *mec1* alleles has shown that the delay of late origin firing by the checkpoint has only limited importance to yeast survival in MMS compared to the maintenance of replication forks. This conclusion is based on the analysis of *mec1-100* and *mec1* Δ yeast, which are both defective in blocking late origin firing in MMS, but only *mec1* Δ is sensitive to MMS (45). The difference observed between these two *mec1* alleles is a 10-fold increase in stalled replication forks in *mec1* Δ cells in comparison to the *mec1-100* cells (62), suggesting that fork stability and return to replication play crucial roles in the S-phase checkpoint.

DNA replication complexes established at origins require the Dfp1 (*S. pombe*)- or Dbf4 (*S. cerevisiae*) dependent kinase (DDK) Hsk1 (*S. pombe*) or Cdc7 (*S. cerevisiae*) for activation (28). Cds1 (*S. pombe*) and Rad53 (*S. cerevisiae*) negatively regulate the DDK, and this may delay late origin firing (13, 29, 55, 60). However, mutations in the DDK components that retain their essential function of DNA replication initiation and checkpoint delay still exhibit hypersensitivity to MMS and

* Corresponding author. Present address: Molecular Physiology and Biophysics, 710 Light Hall, Vanderbilt University-Medical Center, Nashville, TN 37232-8725. Phone: (615) 322-7898. Fax: (615) 322-7236. E-mail: Dewight.williams@vanderbilt.edu.

hydroxyurea (HU) (25, 59), suggesting an additional role for this kinase complex in DNA damage tolerance. The activity of Rad53 (*S. cerevisiae*) kinase is necessary for pol-prim phosphorylation in response to checkpoint activation (18). This phosphorylation may be mediated through activity of the DDK, since it can phosphorylate Pol1p in budding yeast (65), and Rad53 is competent to recruit the DDK to replication origins in budding yeast (14). The *mcl1-1* mutant has a strong genetic interaction with the fission yeast DDK mutant (66). In addition to sharing sensitivity to MMS and decreased sister chromatid cohesion (2), both DDK and *mcl1-1* mutants are partially rescued by deletion of the *cds1* gene but are lethal when *Cds1* is overexpressed or *rad3* is deleted. The temperature-sensitive DDK mutant, the *hsk1-1312* mutant, initiates DNA replication inefficiently at permissive temperatures (55), and this phenotype can be exacerbated by the overexpression of Mcl1p (66). In sum, these results hint that Mcl1p is part of the *Cds1*-Hsk1 regulatory loop, possibly regulating Pol1p functions.

The phenotypes found in the *mcl1-1* and the *ctf4* mutants suggest that Mcl1 and Ctf4 regulate Pol1p. To test whether this interaction between members of the Ctf4 family and Pol1p is conserved in *S. pombe*, we constructed two epitope-tagged versions of Mcl1p for the study of Pol1p interactions. Our data suggest that Mcl1p interacts directly with Pol1p through its N terminus and that this region of Pol1p is sufficient for high-affinity interaction with Mcl1p in vivo during S phase or during DNA replication stress. Furthermore, the *mcl1-1* mutant is acutely sensitive to DNA damage during DNA replication. We also examined the effect that the overexpression of *Cds1p* or mutations in *rad3*, *cds1*, and *hsk1* would have on Pol1p- and Mcl1p-containing complexes arrested in S phase and interpret our data to mean that the Mcl1p-Pol1p interaction is affected by the *Cds1*-Hsk1 checkpoint regulatory loop.

MATERIALS AND METHODS

Yeast strain construction. Genotypes of yeast strains are listed in Table 1. The *mcl1*⁺ gene was tagged with a hexahistidine and a dual myc epitope by subcloning a SalI-BglII fragment (66) from pTOPO4Blunt (Invitrogen, Carlsbad, Calif.), which contained *mcl1*⁺, into SalI-BamHI sites of the multiple cloning site in pREP41x MH vector (8). This dual-epitope-tagged allele was integrated into the chromosomal locus under the control of the no message in thiamine 41x (nmt41x) promoter by first subcloning the nmt41x promoter plus 1 kb of *mcl1*⁺, contained within a PstI-NsiI fragment, into pSport-*ura4*⁺ flanked by 1.2 kbp of the endogenous promoter region of *mcl1*⁺, contained in a SphI-SpeI genomic fragment. Primers 5'-GAATCAGTGGACGAAACCAC-3' and 5'-ATGTTTGTTCATTAATAG-3' were used to amplify the integration cassette. PCR products were gel purified and transformed into haploid 99 cells. Homologous integrants were identified by PCR screening and linkage to *mcl1-1* (data not shown). Construction of an Mcl1-green fluorescent protein (GFP) strain was previously described (66). Strain phenotypes were confirmed by using standard fission yeast procedures (40).

Cell synchronizations and chemical treatments. The reversible, temperature-sensitive arrest of the *cdc10-129* mutation in either an *mcl1*⁺, *mcl1-1*, or *rad3Δ* background were used to synchronize early-log-phase cultures ($A_{595} = 0.3$) in G₁. These cells were arrested by a shift to 36°C for 3 h, either treated with 12 mM HU or 0.02% MMS or mock treated 30 min prior to a temperature shift down to the permissive growth conditions (25°C), which releases the cells into G₁, removed at the times stated, and washed three times. Serial dilution assays were performed by patch plating onto yeast extract medium plus supplements (YES) followed by 3 days of growth at 25°C. Flow cytometry was performed as described previously (4). For an assessment of UV sensitivity, patched cells were dried onto the agar surface and then immediately exposed to 100 J of UVB light/m² in a Stratagene (Stratagene, La Jolla, Calif.)

Two-dimensional DNA gels. Two hundred milliliters of G₁ synchronized cultures was treated with 5 mM HU 30 min prior to release from arrest. Replicating genomic DNA was isolated as described previously (30). A Molecular Dynamics Storm PhosphorImager was used for signal collection, and their ImageQuant 5.1 software was used to quantify total hybridization signal by selection of regions of interest that contained the 1 to 2 N DNA range.

Yeast cellular disruption. Cells (1×10^{10}) were harvested and resuspended in a lysis buffer containing 50 mM Na₂HPO₄, pH 8.0, 150 mM NaCl, 10 mM imidazole, 5 mM NaF, 1 mM NaVO₄, 15 mM β-glycerolphosphate, 2 mM MgCl₂, 0.1% Triton X-100, 1 mM 4-(2-aminoethyl)benzenesulfonyl fluoride HCl, 1 mM phenylmethylsulfonyl fluoride, 10 μM pepstatin, 100 μM leupeptin, 10 U of aprotinin/ml, 10 U of soybean trypsin inhibitor/ml, and 5 mM N-ethylmaleimide. Cells were disrupted by a 30-min burst of agitation at 4°C in a Ribolyser (Bio101, Carlsbad, Calif.) using setting 6.5 in the presence of 0.45-μm-diameter glass beads. This process achieved >90% lysis of cells. Clarification of lysates was performed by centrifugation at 15,000 × g in a Sorvall SS-34 rotor (Dupont, Newtown, Conn.) at 4°C for 30 min.

Chromatin extraction. The procedure used for chromatin extraction was previously described (27).

Pulldown assays. pGT-Pol1p¹¹⁸⁻⁶³⁴ (46), pGT-Pol1p¹¹⁸⁰⁻¹⁴⁰⁵, and pGEX2T (empty) plasmids were expressed in *Escherichia coli* DH5α cells. Bacterial lysates were batch bound to glutathione-Sepharose 4B (GSH-Sepharose) resin (Pharmacia, Uppsala, Sweden), washed with 50 column volumes of phosphate-buffered saline with 0.1 mM phenylmethylsulfonyl fluoride, and stored at 4°C. Clarified yeast lysates containing 2 mg of total protein were mixed with 100 μl of settled glutathione S-transferase (GST) or GST-Pol1p affinity matrices for 1 h at 4°C and then placed into a disposable polycarbonate column, washed with 300 bed volumes of yeast lysis buffer, and then eluted with 1 bed volume of lysis buffer plus 20 mM glutathione.

Strains 592 to 597 were generated from strains 598 to 603 by transformation with pTB19, which contains the first 180 amino acids of Pol1p fused in frame with GFP under its endogenous promoter (12). Fifty-milliliter cultures were grown to mid-log phase in selective medium and harvested. Three milligrams of total protein in clarified lysates was mixed with 25 to 50 μl of a cobalt-immobilized affinity matrix (Talon resin; Clontech, Palo Alto, Calif.) for 1 h at 4°C to bind all available Mcl1-MHP. DNase I treatment of Talon resin-bound Mcl1-MHP complexes was performed at 4°C using 100 U of DNase I for 1 h in the presence of 2 mM MgCl₂. Talon resin was washed with 30 column volumes of lysis buffer, and the bound proteins were eluted with 250 mM imidazole in lysis buffer.

Sucrose gradients. Three milligrams of total protein was layered atop 5 to 15% (wt/vol) sucrose gradients. Sedimentation by centrifugation at 155,000 × g in a SW40 rotor at 4°C for 20 h was done in a Beckman L5 preparative ultracentrifuge. Fractions (22 by 0.5 ml) were collected from the bottom of gradients, with fraction 1 being the bottom of the gradient. Sedimentation velocity for different yeast backgrounds was determined by comparison of the unknown to a standard line, generated by linear regression from the sedimentation velocities of known standards. Protein sedimentation peaks were determined by quantifying band intensities of scanned images of blots with the image analysis software Metamorph (Universal Imaging Corporation, Downingtown, Pa.) to determine the integrated intensity of each band. The mean for the area under each peak was calculated by generating a curve by nonlinear regression with a 95% confidence interval to best fit the data.

Antibodies. Proteins were visualized following sodium dodecyl sulfate-polyacrylamide gel electrophoresis separation by Western blotting and immunodetection. Primary antibodies were detected with horseradish peroxidase secondary antibodies (Sigma, St. Louis, Mo.) and SuperSignal chemiluminescent substrate (Pierce, Rockford, Ill.). Immunoblotting and immunoprecipitations were carried out as described previously (33). 9E10 (monoclonal anti-myc) was used for immunostaining (16), an affinity-purified rabbit anti-myc from Covance (Princeton, N.J.) was used for immunoprecipitation, an affinity-purified chicken anti-Pol1p was used to detect p180 (47), an affinity-purified rabbit antibody raised against the green fluorescent protein was used for immunostaining and immunoprecipitation of GFP fusion proteins (a gift from the Pam Silver lab, Harvard Medical School, Boston, Mass.), and a monoclonal antibody with affinity for GST from BabCo (Richmond, Calif.) was used for immunostaining of GST conjugates.

RESULTS

Repression of *mcl1*⁺ expression in yeast has genetic interactions and chemical sensitivities like those of *mcl1-1*. The screen that identified *mcl1-1* demonstrated a high incidence of

TABLE 1. Yeast strains

Strain	Source	Genotype
53		<i>cdc10-129 leu1-32</i>
99		<i>h⁻ ade6-M210 leu1-32 ura4-D18 his3-D1</i>
546		<i>h⁻ mcl1-1 ade6-M210 leu1-32 ura4-D18 his3-D1</i>
547	S. Sazar	<i>h⁻ mad2Δ::ura4⁺ ade6-M216 leu1-32 ura4-D18</i>
549	J. P. Javazet	<i>h⁻ bub1Δ::ura4⁺ ade6-M216 leu1-32 ura4-D18</i>
551		<i>h⁻ mcl1GFP::ura4⁺ ade6-M210 leu1-32 ura4-D18 his3-D1</i>
553		<i>h⁻ mcl1GFP::ura4⁺ cds1Δ::ura4⁺ ade6-M210 leu1-32 ura4-D18 his3-D1</i>
554		<i>h⁺ mcl1GFP::ura4⁺ nmt1::GSTcds1 LEU2 ade6-704 leu1-32 ura4-D18</i>
555		<i>h⁻ mcl1GFP::ura4⁺ hsk1-1312 ade6-M210 leu1-32 ura4-D18 his3-D1</i>
558		<i>h⁻ mcl1GFP::ura4⁺ cdc25-22 ade6-M210 leu1-32 ura4-D18 his3-D1</i>
561		<i>h⁻ mcl1GFP::ura4⁺ cdc22-M45 ade6-M210 leu1-32 ura4-D18 his3-D1</i>
560		<i>h⁻ mcl1GFP::ura4⁺ cdc10-129 ade6-M210 leu1-32 ura4-D18 his3-D1</i>
562		<i>h⁻ mcl1GFP::ura4⁺ rad3Δ::ura4⁺ ade6-M210 leu1-32 ura4-D18 his3-D1</i>
578		<i>h⁻ mcl1-1 cdc10-129 leu1-32</i>
590	G. Freyer	<i>h⁻ rqh1Δ::ura4⁺ ade6-M210 leu1-32 ura4-D18</i>
591		<i>h⁻ rad3Δ::ura4⁺ cdc10-129 leu1-32</i>
592		<i>h⁻ nmt41x-mcl1-MH::ura4⁺ ade6-M210 leu1-32 ura4-D18 his3-D1</i>
593		<i>h⁻ nmt41x-mcl1-MH::ura4⁺ ade6-M210 leu1-32 ura4-D18 his3-D1 cdc25-22</i>
594		<i>h⁻ nmt41x-mcl1-MH::ura4⁺ ade6-M210 leu1-32 ura4-D18 his3-D1 cdc22-M45</i>
595		<i>h⁻ nmt41x-mcl1-MH::ura4⁺ ade6-M210 leu1-32 ura4-D18 his3-D1 cdc21-M68</i>
596		<i>h⁻ nmt41x-mcl1-MH::ura4⁺ ade6-M210 leu1-32 ura4-D18 his3-D1 cdc10-129</i>
597		<i>h⁻ nmt41x-mcl1-MH::ura4⁺ ade6-M210 leu1-32 ura4-D18 his3-D1 orp1-4</i>
598		<i>h⁻ nmt41x-mcl1-MH::ura4⁺ ade6-M210 leu1-32 ura4-D18 his3-D1/pTB19</i>
599		<i>h⁻ nmt41x-mcl1-MH::ura4⁺ ade6-M210 leu1-32 ura4-D18 his3-D1 cdc25-22/pTB19</i>
600		<i>h⁻ nmt41x-mcl1-MH::ura4⁺ ade6-M210 leu1-32 ura4-D18 his3-D1 cdc22-M45/pTB19</i>
601		<i>h⁻ nmt41x-mcl1-MH::ura4⁺ ade6-M210 leu1-32 ura4-D18 his3-D1 cdc21-M68/pTB19</i>
602		<i>h⁻ nmt41x-mcl1-MH::ura4⁺ ade6-M210 leu1-32 ura4-D18 his3-D1 orp1-4/pTB19</i>
603		<i>h⁻ nmt41x-mcl1-MH::ura4⁺ ade6-M210 leu1-32 ura4-D18 his3-D1 cd1Δ::ura4⁺/pTB19</i>
1123	A. Carr	<i>h⁻ rad26Δ::ura4⁺ ade6-704 leu1-32 ura4-D18</i>
FY865	S. L. Forsburg	<i>h⁻ cds1Δ::ura4⁺ leu1-32 ura4-D18</i>
FY945	S. L. Forsburg	<i>h⁻ hsk1-1312 ade6-M210 leu1-32 ura4-D18</i>
FY1105	S. L. Forsburg	<i>h⁺ rad3Δ::ura4⁺ ade6-M216 leu1-32 ura4-D18</i>

chromosome loss and synthetic lethality with *bub1Δ* but not another spindle assembly checkpoint mutant, *mad2Δ*. In addition, we found that *mcl1-1* was synthetic lethal with *rad3Δ*, *rad26Δ*, *hsk1-1312*, and *rqh1Δ* (*rad12*), indicating that the viability of *mcl1-1* strains depended on DNA damage checkpoints. However, the *mcl1-1* mutant was partially rescued for its slow growth when *cds1* or both *chk1* and *cds1* genes were deleted, demonstrating that the downstream effectors of the checkpoint were dispensable and, in the case of *Cds1p*, deleterious (66). Sequencing of the *mcl1-1* allele revealed a single lesion changing the 124th amino acid from a W to an ochre stop. To ensure that the phenotypes associated with *mcl1-1* were due to decreased protein product from translational read-through as opposed to neomorphic effects arising from the production of the short 124-amino-acid fragment, we examined the growth, genetic interactions, and chemical sensitivities of the mutant with the repressible promoter, *nmt41mcl1-MH* (Table 1). This new allele of *mcl1* produced a protein of predicted size and had no overt growth phenotypes in conditions where the promoter was induced (Fig. 1A), but overexpression of Mcl1 did have genetic interactions with DNA damage checkpoint genes (Table 2), suggesting that the overexpression of Mcl1 is also deleterious. Under promoter-repressed conditions, the *nmt41mcl1-MH* strains had similar growth characteristics and genetic interactions as *mcl1-1* (Fig. 1A and Table 2). After several generations at 25°C, cell cycle-arrested cells were evident (Fig. 1A and C). This phenotype was more pronounced at 36°C, possibly due to the more rapid dilution of excess

Mcl1p upon promoter shutdown through the increased cell division rate at 36°C. Deletion of *mcl1* is lethal to fission yeast (66), so not surprisingly, the repression of *nmt41mcl1-MH* expression for greater than 50 division cycles led to no detectable cell viability in cultures (Fig. 1A).

The *nmt41mcl1-MH* mutant had genetic interactions similar to those of the *mcl1-1* mutant. For instance, the *bub1Δnmt41mcl1-MH* mutant was unable to grow with *nmt41mcl1-MH* repressed, whereas the *mad2Δnmt41mcl1-MH* mutant grew like the *nmt41mcl1-MH* mutant alone (Fig. 1B and Table 2). *nmt41mcl1-MH* was also synthetic lethal with *rad3Δ*, *rad26Δ*, *rqh1Δ*, and *hsk1-1312* under promoter-repressed conditions (Table 2). In attempts to recover viable double mutant spores from these various genetic backgrounds, we performed crosses and plated spores onto selective medium lacking thiamine in the hope that the expression of Mcl1-MHp would allow recovery of the DNA damage checkpoint double mutants. Still, no double mutant strains were recovered from these crosses, demonstrating that these mutations are synthetic lethal with *nmt41mcl1-MH*. In particular, the *hsk1-1312* mutant crossed to *nmt41mcl1-MH* strains consistently produced asci with five to eight spores, suggestive of meiotic segregation failures. In contrast, *mcl1-GFP* which is expressed from the endogenous promoter showed no genetic interactions or growth defect with any of these mutant combinations.

The *nmt41mcl1-MH* strain also showed a sensitivity to growth in the continual presence of 0.0025% MMS, 5 mM HU, and 10 mg of thiabendazole (TBZ)/ml (Fig. 1C). *nmt41mcl1-MH* expression was repressed by thiamine addition to cultures 18 h

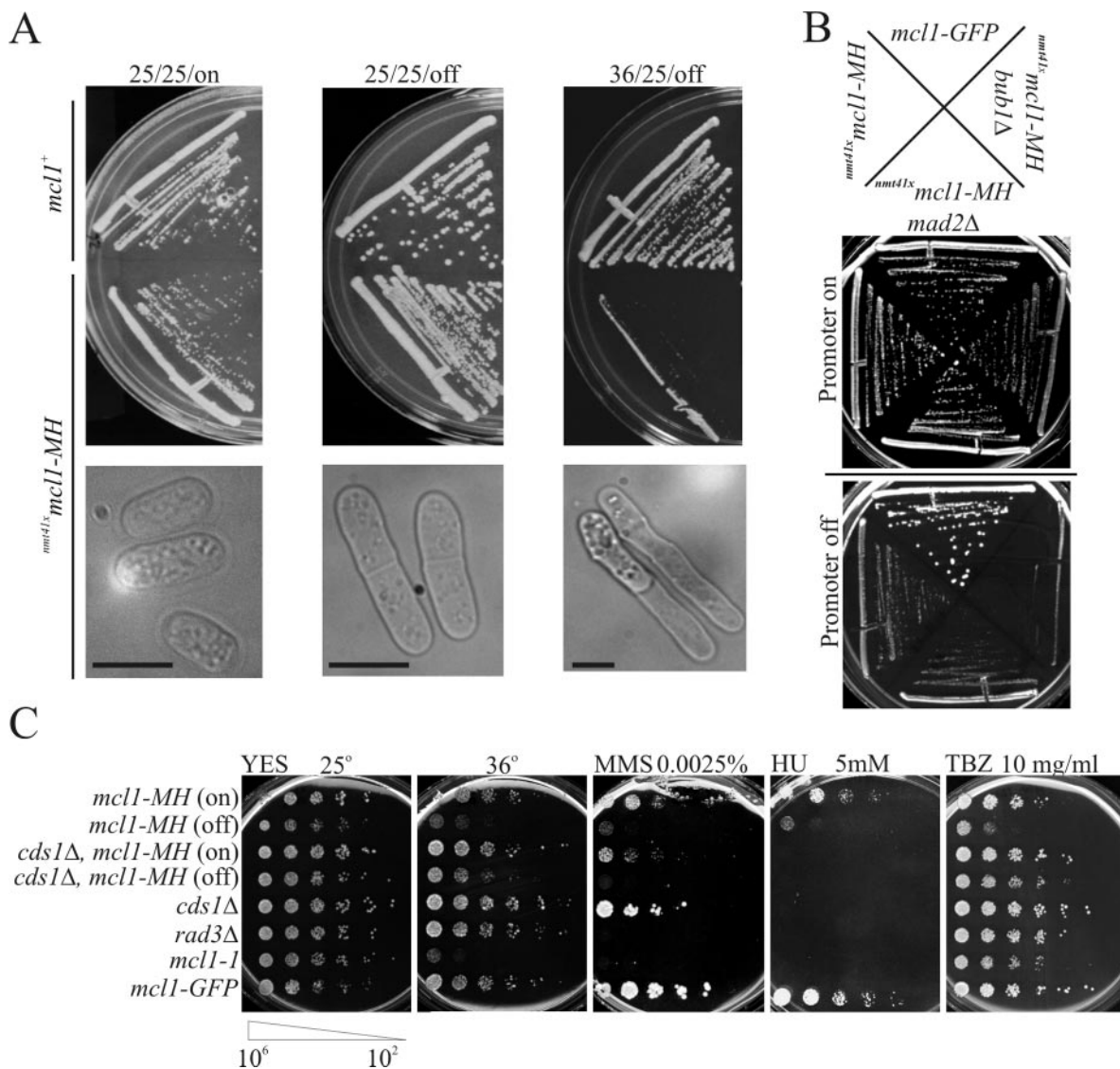


FIG. 1. The *nmt41x mcl1-MH* mutant is phenotypically similar to the *mcl1-1* mutant. (A) Growth of the *nmt41x mcl1-MH55* strain and the parental *mcl1*⁺ strain at 25°C for 25 generations in selective medium containing no thiamine (25/25/on), with 10 mM thiamine to repress *nmt* gene expression (25/25/off), or at 36°C (36/25/off). The lower panel is a phase-contrast light microscope image of *nmt41x mcl1-MH55* cells from the liquid culture prior to plating (bar in phase-contrast images represent 5 μm). (B) Recovered double mutant *nmt41x mcl1-MH bub1Δ* and *nmt41x mcl1-MH mad2Δ* strains were struck onto selective media containing 0 (on) or 10 (off) mM thiamine to examine the differences in the genetic interactions between *nmt41x mcl1-MH* and the two spindle checkpoint mutations at permissive temperature of 25°C. (C) Cultures of *nmt41x mcl1-MH* (603), *cds1Δ* (FY865), *rad3Δ* (591), *mcl1-1* (546), and *mcl1-GFP* (551) cells were grown for 25 generations in selective media and then split into medium without (on) or with (off) 10 mM thiamine for 6 generations before plating on YES agar plates (a thiamine-enriched medium) containing 0.0025% MMS, 5 mM HU, or 10 mg of TBZ/ml. Cells were serially diluted 1:5 from 10⁶ to 10² cells/ml.

prior to plating (Fig. 1C, “off” rows). Promoter repression of this duration depletes Mcl1-MHp to levels undetectable by immunoblotting of cellular lysates (Fig. 2D). Under these promoter-repressed conditions, *nmt41 mcl1-MH* mutant drug sensitivities were similar to those of the *mcl1-1* mutant (Fig. 1C). Deletion of *cds1*⁺ in the *nmt41 mcl1-MH* cell line rescued the strain’s sensitivity to TBZ and the slower growth induced by the repression of *mcl1* gene expression. Induction of this promoter did not, however, produce a truly wild phenotype. When Mcl1-MHp was expressed, the *nmt41 mcl1-MH* mutant showed a 125-fold greater sensitivity to MMS and 25-fold more sensitiv-

ity to HU and TBZ than the *mcl1-GFP* mutant, which grows with a wild-type phenotype.

Mcl1p interacts with the N terminus of Pol1p both in vitro and in vivo. Two epitope-tagged Mcl1 proteins (diagrammed in Fig. 2A) were highly enriched in material recovered from yeast cellular lysates bound to an affinity matrix composed of an N-terminal Pol1 protein fragment fused to GST (GST-NT in Fig. 2B and C). This protein fragment contains amino acids 118 to 634 of Pol1p (47). None of these tagged alleles of Mcl1p interacted strongly with the C-terminal GST-Pol1p protein chimera (GST-CT in Fig. 2B and C) or GST (Fig. 2C). Such

TABLE 2. Genetic interactions^a

Mutation	Function	Interaction with			
		<i>mcl1-1</i>	<i>mcl1-GFP</i>	<i>nms41 mcl1-MH</i>	
				On	Off
<i>mad2Δ</i>	Spindle assembly checkpoint	NI	NI	NI	NI
<i>bub1Δ</i>	Spindle assembly checkpoint kinase	SL	NI	S	SL
<i>rad3Δ</i>	DNA damage checkpoint kinase	SL	NI	SL	SL
<i>rad26Δ</i>	Rad3 interaction protein	SL	NI	SL	SL
<i>rad9Δ</i>	DNA damage checkpoint (PCNA like)	S	NI	NI	S
<i>hsk1-1312</i>	S-phase initiation kinase	SL	NI	ML	ML
<i>cds1Δ</i>	Transducer kinase for S-phase	PR	NI	NI	PR
<i>rqh1Δ</i>	RecQ helicase homolog	SL	NI	SL	SL
<i>pol1-1</i>	DNA polymerase-α	NI	NI	NI	NI
<i>rad22Δ</i>	Rad52 homologue	NI	NI		
<i>rph51Δ</i>	Rad51 homologue	ML	NI		
<i>rph54Δ</i>	Rad54 homologue	ML	NI		

^a NI, no interaction; S, synthetic; SL, synthetic lethal; PR, partial rescue; and ML, meiotic lethal.

GST pulldown assays from whole-cell lysates demonstrate a high-affinity interaction between Mcl1p and the N terminus of Pol1p.

An *in vivo* interaction between the N terminus of Pol1p and Mcl1-MHp was tested by expression of the first 180 amino acids of Pol1p C-terminally fused to GFP (Fig. 2B, bottom) and expressed under the regulation of its endogenous promoter from a plasmid (pTB19) in *nms41 mcl1-MH* cells. Purification of Mcl1-MHp with Talon resin recovered only a fraction of the GFP-NT chimera (Fig. 2B) from cell lysates when cells were grown in the absence of 10 mM thiamine (Fig. 2D, ON) but did not recover any detectable GFP-NT when the expression of Mcl1-MHp was repressed by 10 mM thiamine (Fig. 2D, OFF). Because DNA might have mediated this weak interaction, we digested the purified material while it was still on the Talon beads with DNase I, followed by extensive washes (Fig. 2D). This treatment was not sufficient to disrupt the weak Mcl1-MHp interaction with the GFP-NT protein fragment. Expression of GFP with Mcl1-MHp does not recover GFP with Mcl1-MHp, demonstrating that the Pol1p fragment interaction was not induced by nonspecific interaction between GFP and Mcl1-MHp.

The contrast between strong *in vitro* and weak-appearing *in vivo* interactions between Mcl1p and the N-terminal Pol1p fragments led us to hypothesize either that these different protein fragments had different affinities for Mcl1-MHp or that the *in vivo* interaction was regulated, such that only a fraction of cells contained Pol1-NTp/Mcl1-MHp complexes. Since a similar observation had been reported for reciprocal immunoprecipitation of Ctf4p and Pol1p from budding yeast cell lysates, we looked for cell cycle dependence for this interaction. Cell lysates arrested by the mutations *cdc25-22* (G₂), *cdc22-M45* (S phase), *cdc21-M68* (S), or *orp1-4* (pre-S) were used in this analysis (Fig. 2E). In G₂ and pre-S-phase arrests (*cdc25-22* and *orp1-4*, respectively), the majority of the GFP-NT remained unbound to Mcl1-MHp recovered by cobalt-immobilized resin, but during S phase nearly all of the GFP-NT in the cellular lysate was recovered with the Mcl1-MHp. Surprisingly, a similar analysis of the N-terminally-tagged Mcl1-MHp failed to detect any direct interaction with endogenous Pol1p (data not shown), but immunoprecipitation of the C-terminally-

tagged Mcl1-GFP does recover endogenous Pol1p (see Fig. 6B).

The *mcl1-1* mutant is sensitive to DNA damage specifically during G₁/S phase. To assess the *mcl1-1* mutant's response to perturbed DNA replication, we used the *cdc10-129* mutation and a temperature shift to the restrictive conditions to arrest cells in G₁, followed by release into permissive conditions to observe synchronous DNA replication in the presence of HU or MMS or exposure to UV irradiation. Since the *mcl1-1* mutant is also temperature sensitive, we tested for any effects of our temperature shift regimen on DNA replication and viability in the absence of treatment in the *cdc10-129* backgrounds. Like *mcl1*⁺ and *rad3Δ* mutants, the *mcl1-1* mutant had increased DNA fluorescence in flow cytometry at 60 min and reached 2C DNA content by 120 min with no detectable loss in relative viability upon return to the permissive temperature (Fig. 3, panels labeled "YES"). This result demonstrates that the *cdc10-129* arrest point precedes the essential point of Mcl1 function for this experiment, so our double mutant can be taken as synchronized at the *cdc10-129* restriction point. In the presence of either HU or MMS, the *cdc10-129 mcl1*⁺ mutant showed no significant DNA content increase (Fig. 3A, two right histograms) and retained high viability (Fig. 3A, panels below histograms), demonstrating that DNA replication was strongly inhibited in these cells by both compounds. In four independent experiments, however, the *cdc10-129 mcl1-1* and *cdc10-129 rad3Δ* mutants consistently showed a dramatic decrease in relative cellular viability in the presence of HU and MMS. This decrease in viability was consistently coincident with the normal timing of DNA replication onset (Fig. 3B and C). Examination of the *cdc10-129 mcl1-1* and *cdc10-129 rad3Δ* strain cytology demonstrated that the *cdc10-129 mcl1-1* mutant does not progress into mitosis in HU and MMS, unlike the *cdc10-129 rad3Δ* mutant (data not shown), so the *mcl1-1* mutation is not defective in checkpoint cell cycle arrest. It follows that the increased sensitivity is most likely due to an abnormal intra-S-phase response to DNA replication perturbation. Close examination of the MMS DNA content in the *mcl1-1* strain showed a slight but significant and consistent increase in DNA content when compared to the *mcl1*⁺ controls. Further support of this S-phase-specific sensitivity was found upon expos-

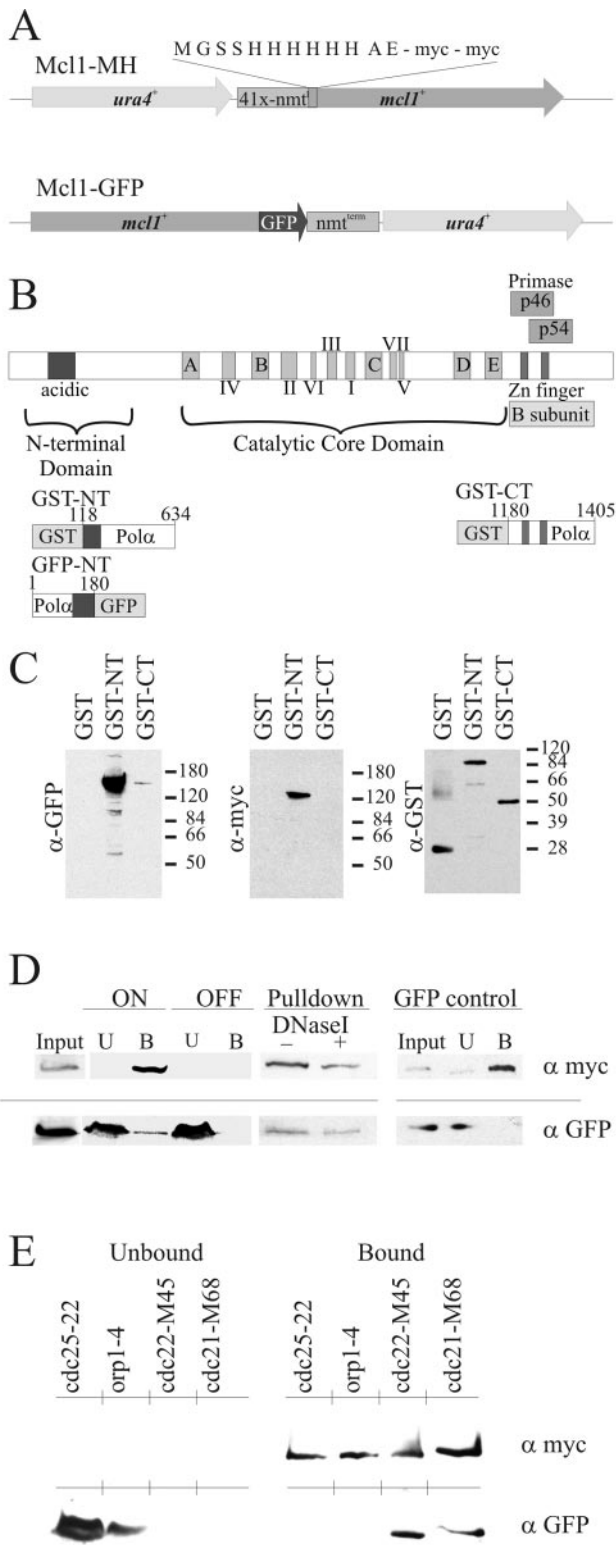


FIG. 2. Mcl1p interacts with N-terminal fragments of Pol1p. (A) Schematic representation of the two epitope-tagged alleles of *mcl1* (strains 551 and 589) used in this study. (B) Schematic representation of the polymerase α holoenzyme showing the three conserved domains of the eukaryotic Pol1 (p180): an acidic N terminus, a central deoxynucleotide transferase catalytic core composed of seven B-polymerase as well as five polymerase α conserved sequences, and the C-

terminal Zn finger domain with B subunit and primase association presented. In the lower panel, the two bacterially expressed GST-Pol1p fragments used for in vitro interaction studies presented in panel C and a fission yeast-expressed Pol1-GFP protein fragment used for in vivo interaction studies presented in panels D and E are shown. (C) Western blot analysis of GST pull-downs from yeast lysates containing Mcl1-GFP (left) or Mcl1-MHp (center) with the various GST proteins (right). The epitope-tagged Mcl1 proteins strongly interact with the GST-NT fragment (center lanes) but not the GST or GST-CT proteins (right and left lanes). (D) Mcl1-MHp interacts in vivo with a small fragment of Pol1p tagged with GFP (GFP-NT). Yeasts were grown in conditions where the *nmt* promoter of *mcl1-MH* was either induced (ON) or repressed with thiamine (OFF). The six-His-tagged Mcl1-MHp was recovered with cobalt-immobilized agarose resin (Talon). Mcl1-MHp interaction with GFP-NT was not disrupted by DNase I digestion of Talon-bound material. Additionally, no interaction was seen between Mcl1-MH and GFP alone. (E) Cell cycle restriction points for the temperature-sensitive *cdc25-22* (G_2 arrest of strain 596), *orp1-4* (pre-S arrest of strain 599), *cdc22-M45* (early S arrest of strain 597), or *cdc21-M68* (mid-S arrest of strain 598) mutants were used to test for a cell cycle-dependent interaction between Mcl1-MHp and GFP-NT. Only those cells arrested in S phase (flow cytometry not shown) had enrichment of GFP-NT in the Mcl1-MHp pull-down with Talon resin.

ing the *cdc10-129 mcl1-1* mutant to 100 J of UVB light/m² prior to or during DNA replication. This step leads to a significant loss of viability, whereas when it is done following DNA replication the strain appears far less affected (Fig. 3C, panel labeled "UV"). This result differs from our original observation, where *mcl1-1* cells exposed in log phase showed little sensitivity to this dosage of UVB irradiation compared to the wild type (66). This sensitivity may have been previously overlooked because two-thirds of the fission yeast cell cycle is spent in G_2 .

Replication forks appear stable and persistent in *mcl1-1* cells under conditions of mild replication stress. Our results suggest that *mcl1*⁺ is important for replication stress. Given the recent evidence that replication fork stability is a major factor in yeast survival of replication stress, we examined replication fork structure by two-dimensional gel analysis using the same three strains as described above and identical synchronization procedures but with release into 5 mM HU. This concentration of the ribonucleotide reductase inhibitor slows rather than completely blocks DNA replication, but it still leads to appreciable cell death in the *mcl1-1* mutant cell line (Fig. 4A). We examined replication at the *ars2-1* chromosomal locus, an early firing origin that remained active during this treatment.

DNA replication intermediates in *cdc10-129 mcl1*⁺ cells were resolved by two-dimensional gel analysis as the X line and bubble arc at 60 min after G_1 release, and a Y arc becomes prominent by 120 min after release (Fig. 4C, left panels, and D). In similarly treated *cdc10-129 rad3 Δ* cells, similar replication forks were detected at *ars2-1* at 60 and 120 min but appeared to accumulate at the 240-min time point. The *rad3 Δ* strain reached a near 2C DNA content more rapidly than *cdc10-129 mcl1*⁺ or *cdc10-129 mcl1-1* cells (Fig. 4A), and cells in the culture began entering mitosis with replication forks still present at 240 min.

An X-DNA line that is indicative of four-way or hemicatenae structures was present in the *cdc10-129 rad3 Δ* and *cdc10-*

terminal Zn finger domain with B subunit and primase association presented. In the lower panel, the two bacterially expressed GST-Pol1p fragments used for in vitro interaction studies presented in panel C and a fission yeast-expressed Pol1-GFP protein fragment used for in vivo interaction studies presented in panels D and E are shown. (C) Western blot analysis of GST pull-downs from yeast lysates containing Mcl1-GFP (left) or Mcl1-MHp (center) with the various GST proteins (right). The epitope-tagged Mcl1 proteins strongly interact with the GST-NT fragment (center lanes) but not the GST or GST-CT proteins (right and left lanes). (D) Mcl1-MHp interacts in vivo with a small fragment of Pol1p tagged with GFP (GFP-NT). Yeasts were grown in conditions where the *nmt* promoter of *mcl1-MH* was either induced (ON) or repressed with thiamine (OFF). The six-His-tagged Mcl1-MHp was recovered with cobalt-immobilized agarose resin (Talon). Mcl1-MHp interaction with GFP-NT was not disrupted by DNase I digestion of Talon-bound material. Additionally, no interaction was seen between Mcl1-MH and GFP alone. (E) Cell cycle restriction points for the temperature-sensitive *cdc25-22* (G_2 arrest of strain 596), *orp1-4* (pre-S arrest of strain 599), *cdc22-M45* (early S arrest of strain 597), or *cdc21-M68* (mid-S arrest of strain 598) mutants were used to test for a cell cycle-dependent interaction between Mcl1-MHp and GFP-NT. Only those cells arrested in S phase (flow cytometry not shown) had enrichment of GFP-NT in the Mcl1-MHp pull-down with Talon resin.

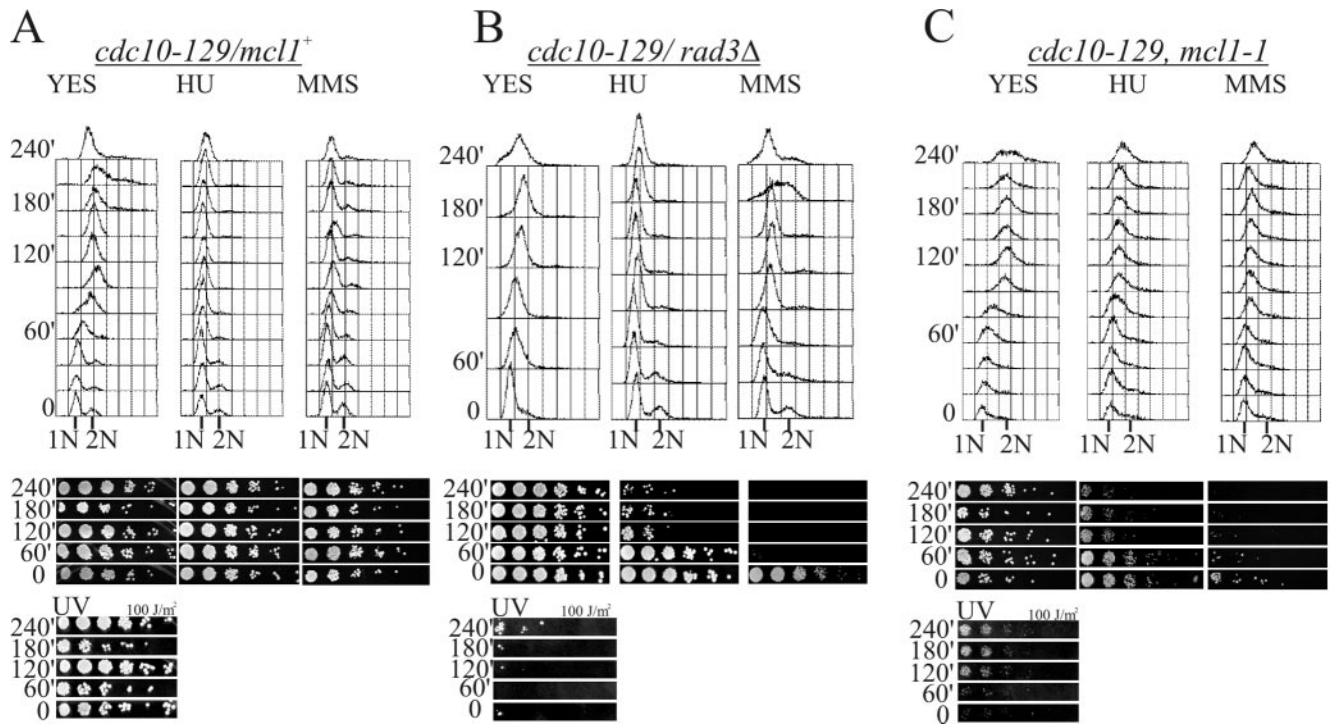


FIG. 3. *mcl1-1* mutants are sensitive to DNA damage specifically in S phase. (A) Cultures of *cdc10-129* cells (strain 53) were arrested for 3 h at 36°C and then released into either YES, YES with 12 mM HU, or YES with 0.02% MMS. Cells were collected to determine DNA content by flow cytometry (top row of three panels) or relative viability, as determined by serial dilution plating (middle row of panels). Cells plated from untreated cultures were also irradiated with 100 J of UV light/m² at given time points (bottom panels). (B and C) *cdc10-129 rad3Δ* cells (strain 591) and *cdc10-129 mcl1-1* cells (strain 578), respectively, were treated as described above. Data presented is representative of four independent experiments.

129 backgrounds at 60 and 120 min (Fig. 4C, open arrowhead). Such an X line is a natural feature of normal origin activation in yeast (30, 49, 50, 56). In *S. pombe*, it is dependent on DNA recombination (54). Both this feature and a bubble arc are not detected in the *cdc10-129 mcl1-1* two-dimensional gel analysis. Although the apparent rates of bulk DNA content increase, as seen by flow cytometry, were similar in *cdc10-129 mcl1+* and *cdc10-129 mcl1-1* cells, the total signal obtained at the *ars2-1* locus remained nearly constant in the *mcl1-1* strain, whereas it doubled in both control strains. It is possible that replication failed to initiate from this region in *mcl1-1* cells but progressed slowly into this locus and stalled in some cells. Unfortunately, analysis of a number of other autonomously replicating sequences (*ars-727*, *ars2-2*, centromeres, telomeres, and *ars3001*) also failed to detect active origins in *mcl1-1* under similar conditions. Since a similar poor origin activation phenotype is found in the recombination mutants *rad22Δ*, *rph51Δ*, and *rph54Δ* (54), we tested the *mcl1-1* mutant's genetic interactions with these two null mutants. We found that *mcl1-1* was lethal with both *rph51Δ* and *rph54Δ*. However, *mcl1-1* showed no overt interaction with *rad22Δ*, such as poor growth or depression in restrictive temperature (Table 2).

Binding of Mcl1-GFP to chromatin during HU arrest is dependent on Hsk1 kinase activity. Mcl1-GFP is chromatin bound during G₁, but it is progressively released as cells move from S phase into G₂ (66). Upon HU arrest, a large fraction of Mcl1-GFP is retained in the nucleus following cell wall disruption and detergent extraction, suggesting that it is tightly bound

to chromatin (Fig. 5A, B, and E, lane 1). Using a previously described chromatin extraction method, we looked at Mcl1-GFP nuclear retention in HU-treated cells lacking Cds1, Rad3, or Hsk1 kinase activities and when Cds1p was overproduced from a chromosomal *nmr1**GST-cds1* gene (6). The loss of either Rad3p or Cds1p from the Mcl1-GFP cells had no effect on nuclear retention of GFP fluorescence during HU arrest (Fig. 5A, C, and E, lane 2). Retention was lost, however, in *hsk1-1312* cells shifted to the restrictive temperature for 3 h after HU arrest (Fig. 5A, D, and E, lane 3). Retention of Mcl1-GFP in the nucleus during HU arrest was also lost by a high level of Cds1 kinase expression (Fig. 5A).

S-phase checkpoint kinases can affect Mcl1-GFP endogenous complexes. The sedimentation velocity of Mcl1-GFP during HU arrest, a condition when the above-mentioned mutant kinases are normally activated, was measured to assess the effect of these enzymes on Mcl1-GFP protein complexes (Fig. 6A). Loss of Cds1p from HU-arrested Mcl1-GFP cells produced a slight sedimentation velocity change (a mean sedimentation velocity of 14.1 S compared to 14.4 S in *cds1+* cells). In contrast, loss of either Rad3 (*rad3Δ*) or Hsk1 (*hsk1-1312* at 36°C), as well as overexpression of Cds1 (*nmr1**GST-cds1*), caused Mcl1-GFP to sediment significantly more slowly (13, 13.6, and 11 S, respectively). These sedimentation velocities were calculated from the sedimentation profiles assuming a Gaussian distribution of material, but in the *hsk1-1312* and *rad3Δ* mutant backgrounds the sedimentation profiles included either an exaggerated trailing fraction or a secondary peak. Thus, the ob-

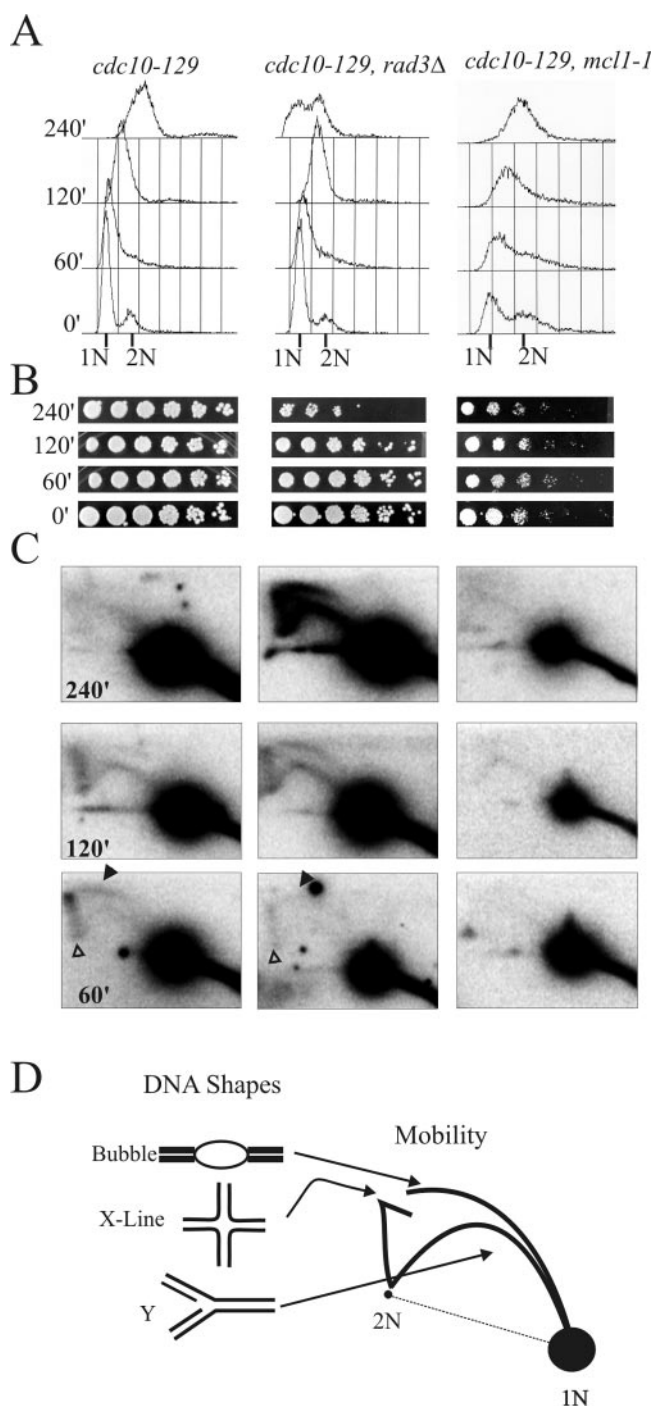


FIG. 4. DNA replication forks at *ars2-1* in *mcl1-1* mutants examined during replication stress are stable and persistent. The three *cdc10-129* strains shown in Fig. 3 were arrested at 36°C and released into 5 mM HU to induce replication stress. Genotypes of strains are given at the top of each column, and each row is labeled from the corresponding time points. (A) Flow cytometric analysis of DNA content in cells released into 5 mM HU. Cytology taken through the experiment showed that most cells entered mitosis by 240 min, except for *mcl1-1* cells, which appeared cell cycle arrested at this time point (data not shown). (B) Relative viability was assessed in serial plating of cultures at each time point. (C) Southern blot analysis of 10 μ g of total DNA by two-dimensional gels probed for *ars2-1* sequences (an early firing origin). Quantification of total signal with Molecular Dynamic ImageQuant 5.1 shows that the hybridization signal increases twofold

served changes in sedimentation velocities probably represent the real change in Mcl1-GFP sedimentation to only a limited extent. Most likely, the sedimenting material breaks into two distinct populations.

To determine whether the observed changes in mobility represented a loss of Pol1p from these Mcl1p complexes, we used a high-affinity antibody to GFP to precipitate Mcl1-GFP from the sucrose gradient fractions. Immunoprecipitation of Mcl1-GFP from fraction 9 coprecipitates Pol1p from all genetic backgrounds except *nmr1 GST-cds1*, which contained no Mcl1-GFP in fraction 9 (Fig. 6B, top panels). Pol1p also precipitated with Mcl1-GFP from the trailing fractions of *rad3Δ* and *cds1Δ*, indicating that the mobility differences observed in these mutants were not due to a loss of Pol1p interaction. In contrast, the slower-sedimenting material in *hsk1-1312* and *nmr1 GST-cds1* fractions contained no detectable Pol1p (Fig. 6B, bottom panels), suggesting that in these backgrounds the association between Pol1p and Mcl1-GFP is weaker than in the other conditions. To test this result in a different way, we used the GST-Pol1NT¹¹⁸⁻⁶³⁴ bound to GSH-Sepharose to collect Mcl1-GFP from 3 mg of total protein in whole-cell extracts from the above arrested strains. This technique also showed that Mcl1-GFP interacts with Pol1p in the *mcl1-GFP*, *cds1Δ*, and *hsk1-1312* backgrounds. It was not, however, present when GST-Cds1p was overexpressed. This result does not appear to be due to the displacement of GST-Pol1NT from the GSH-Sepharose, since the protein is readily detected in the recovered resin along with Mcl1-GFP.

DISCUSSION

Mcl1p belongs to a family of conserved Pol1p accessory factors. Both Ctf4p from budding yeast and Mcl1p from fission yeast interact with Pol1p, suggesting that this is an evolutionarily conserved interaction. Similar proteins have been studied in *Aspergillus nidulans* and *Neurospora crassa* (sepB), humans, and *Xenopus laevis* (AND-1 proteins), and possible homologues have been identified by genome sequencing projects for *Drosophila melanogaster*, *Caenorhabditis elegans*, and *Arabidopsis thaliana* (22, 31, 38, 66), suggesting that a family of eukaryotic Pol1 accessory proteins has been identified. This family is distinguished from the myriad of other WD domain-containing proteins by a highly conserved series of three novel sequence domains (66). WD domains are common protein-protein interaction modules that provide a platform for protein complex formation, suggesting that this family may play a role in regulating polymerase α protein complexes. In the vertebrate homologues, this family also contains a high-mobility group protein type B motif that has been shown to have affinity for X-DNA structures (31).

in the *cdc10-129* (3×10^5 to 6×10^5 counts) and *rad3Δ* (3×10^5 to 5.5×10^5 counts) strains but not the *mcl1-1* strain (2×10^5 to 2.4×10^5 counts). Filled arrowheads mark the bubble arc, and open arrowheads mark the X line. (D) Diagrammatic representation of two-dimensional DNA gel patterns showing how autonomously replicating sequence DNA structure relates to mobility in two-dimensional gel electrophoresis, which is adapted from <http://fangman-brewer.genetics.washington.edu/2Dgel.html>.

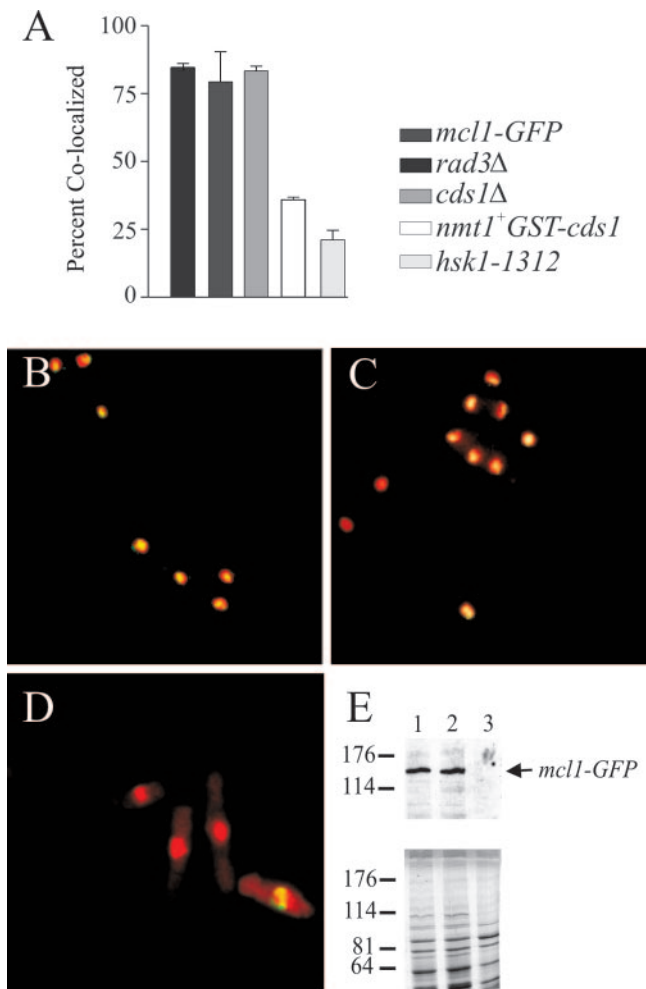


FIG. 5. Hsk1 and Cds1 affect the localization of Mcl1p to chromatin during HU arrest. (A) The percentage of cells that retained Mcl1-GFP in association with chromatin following chromatin extraction procedures is plotted in the histogram, with error bars representing standard error of the mean from four experiments. Cells were at 36°C for 3 h, and cell cycle arrests were confirmed by flow cytometric quantification of DNA content for each experiment (data not shown). (B, C, and D) Representative deconvolved fluorescence images of *mcl1-GFP* (strain 551; panel B), *cds1Δ mcl1-GFP* (strain 553; panel C), and *hsk1-1312 mcl1-GFP* (strain 555; panel D) cells are shown after chromatin extraction. DNA stained with Hoechst 33258 is false colored red, Mcl1-GFP is in green, and colocalized signal appears yellow. (E) To quantify the remaining Mcl1-GFP in the chromatin fraction, the postextraction chromatin-containing material was separated by sodium dodecyl sulfate–8% polyacrylamide gel electrophoresis and transferred by Western blotting for immunodetection of Mcl1-GFP: lane 1, *mcl1-GFP*; lane 2, *cds1Δ*; and lane 3, *hsk1-1312*. The bottom panel is Coomassie-stained gel loaded identically for a loading control, since protein expression appears altered in the *hsk1* mutant background.

Direct interaction between Mcl1p and Pol1p. We have shown that the N terminus of Pol1p exhibits high-affinity binding to two epitope-tagged alleles of Mcl1p. Tandem affinity purification of the Mcl1-MHp with immobilized metal affinity chromatography followed by affinity for the Pol1¹¹⁸⁻⁶³⁴-GST recovered a single Mcl1-MHp band on silver-stained gels, demonstrating that this interaction can be direct (our unpub-

lished observations). Although we have not detected a direct interaction between Mcl1-MHp and endogenous Pol1p, this may have been due either to a masking of the relevant epitope and/or to overexpression of Mcl1-MHp. Relevant interactions were readily detected between Mcl1-GFP and endogenous Pol1p as well as Pol1NT protein fragments and Mcl1-MHp. These fragments that interact with Mcl1p all contain a conserved acidic domain of low complexity (Fig. 2B). Studies of mice and yeast have mapped binding sites for the two primase and the regulatory B subunits to the conserved C-terminal Zn finger domain of Pol1 (mouse p180) (5, 39). The C-terminal Zn finger domain had only very weak to no interaction with Mcl1-GFP and no interaction with Mcl1-MHp (Fig. 1C). Based on this and a lack of S-M checkpoint defects in *mcl1* mutants, we believe that the association of Mcl1p with Pol1p is probably not regulating primase and B subunit association or activities, although we have not assayed for differences in Pol1p association with other members of the polymerase α -primase tetramer.

The acidic, N-terminal domain of Pol1p that binds to Mcl1p is homologous to the region of mammalian p180 that binds to the simian virus 40 viral replication initiator protein, T antigen, which acts as a dodecameric replicative helicase for viral replication (10). Thus, Mcl1p may regulate the association of replication fork complexes with Pol1p. In budding yeast, the binding of Ctf4p to Pol1p is mutually exclusive with the Pob3/Cdc68 heterodimeric protein complex (67). The Pob3/Cdc68 protein complex in budding yeast, as well as a homologous complex in *X. laevis* and humans, is important for DNA unwinding and chromatin remodeling. Such activity appears to be essential for polymerase access to the DNA template, since loss or inhibition of this complex blocks DNA replication initiation and alters transcription (19, 42). In light of the *mcl1-1* and *ctf4Δ* defects in chromatid cohesion and the ability of Mcl1p to exacerbate DNA replication initiation when overexpressed, it appears that this family could regulate the association of important chromatin modifiers with Pol1p. Swi6 is a heterochromatin protein 1 equivalent that has recently been shown to bind to Pol1p in fission yeast (1). This interaction is essential for heterochromatin formation at telomeres and centromeres and for mating type information silencing, as well as for recombination and chromatid cohesion. It is very interesting, then, that Mcl1p, Pol1p, and DDK affect sister chromatid cohesion (1–3). Likewise, Mcl1p, Pol1p, and checkpoint proteins affect telomere length regulation in fission yeast (9, 36). These phenotypes taken together suggest that the Mcl1p-Pol1p interaction may affect locus-specific alterations of chromatin and may be affected by the functions of S-phase regulatory kinases.

Possible regulation of the interaction between Mcl1p and Pol1p. Mcl1p interaction with chromatin and Pol1p-containing complexes can be partially disrupted by loss of Hsk1 kinase or overexpression of Cds1 kinase. The Hsk1/Cdc7 family of kinases phosphorylates a number of replication proteins, including Pol1p and Swi6p, in vitro (34, 65). It is active only during S phase because of its dependence on the cycling cofactor Dfp1/Dbf4p (7, 43). Data from both budding and fission yeast support a role for the DDK in three pathways: replication initiation, DNA damage tolerance, and meiotic DNA recombination (26, 44, 59). We previously found that overexpression of Mcl1-GFP can lead to an increased accumulation of cells

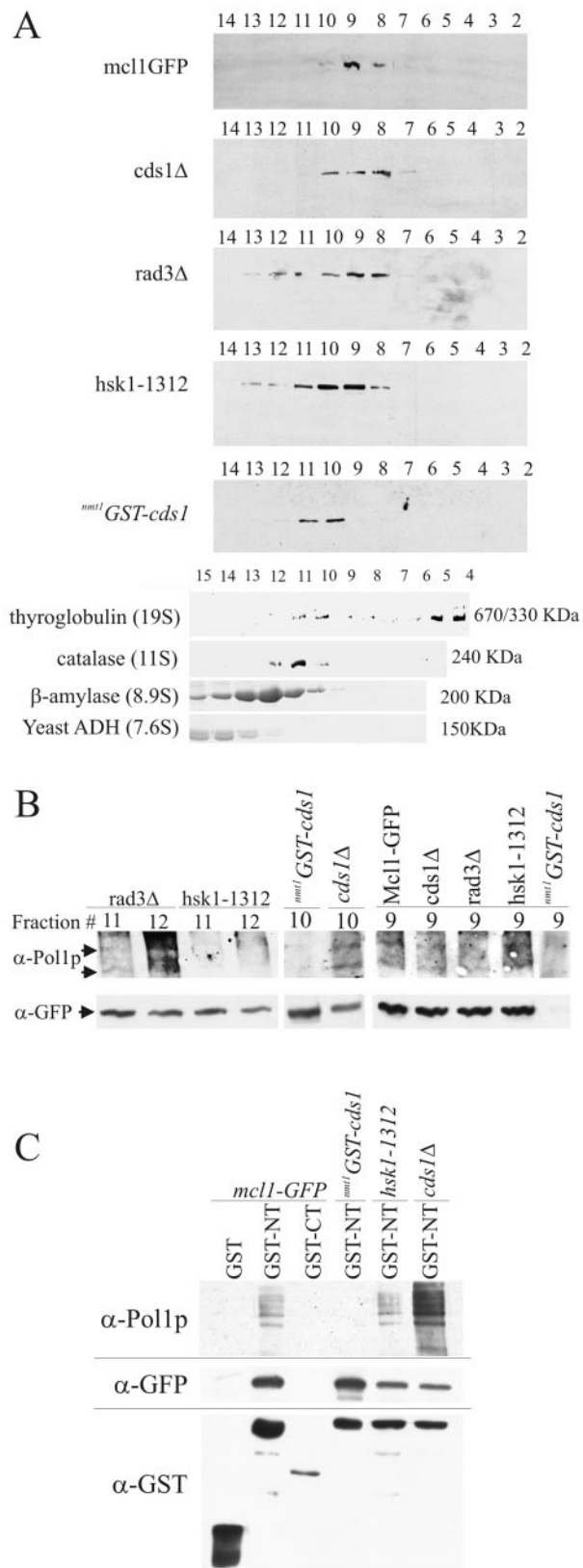


FIG. 6. Checkpoint kinases affect Mcl1p complexes. (A) Sucrose gradient sedimentation of Mcl1-GFP from nonmutant (*mcl1*-GFP), *cds1*Δ, *rad3*Δ, and *hsk1*-1312 cells arrested with 12 mM HU and cells

with a G₁- to mid-S-phase DNA content, especially in the *hsk1*-1312 mutant background (66), but the exact nature of this arrest remains enigmatic. Both DDK and Mcl1 mutants show similar sensitivities to HU and MMS, as well as being defective in centromeric cohesion (60). Finally, a cross between the *mml1* *mcl1*-MH and *hsk1*-1312 mutants appeared to be meiotically lethal, since asci produced from the mating of these two strains contained five to eight spores, instead of the usual four spores (our unpublished observations), suggesting that this *hsk1* mutant is particularly sensitive to altered Mcl1p expression levels. Together, these data imply that DDK and Mcl1p may share a regulatory pathway.

Hsk1 is a target of Cds1 phosphorylation, as is the cycling subunit, Dfp1. Phosphorylation of either DDK component down-regulates Hsk1/Dfp1 kinase activity (29, 55, 59). This may suggest that the overexpression of Cds1p is equivalent to inactivation of Hsk1 in our experiments. One surprising result was the ability of the Cds1 null mutation to rescue the TBZ sensitivity of the thiamine-repressed *mml1* *mcl1*-MH strain, which would suggest that Cds1 exacerbates the cohesion defects of *mcl1* mutants, possibly through down-regulation of Hsk1. It is interesting that recent work with budding yeast shows a connection between Rad53 and cohesion that was uncovered by genetic interaction with Ctf4 mutants (64). Although intriguing, we believe that the interaction between Cds1p, Hsk1p, and Mcl1p is more complex, because the overexpression of even a kinase dead version of Cds1p is toxic to *mcl1*-1 strains (66), suggesting that Cds1 is a molecular poison in the *mcl1*-1 mutant. Thus, Cds1p may have multiple intersecting roles that exacerbate replication defects in Mcl1 mutants. Certainly, the overexpression of Cds1p creates a condition where it is difficult to detect interaction between Pol1p from Mcl1p.

Mcl1p is important for S-phase response to DNA damage. The *mcl1*-1 mutant has a higher sensitivity to UV DNA damage during S phase than had previously been found in cycling cells (Fig. 1 and 3). In light of this strain's increased sensitivity to HU and MMS, we interpret our observation as a result of a defect in an S-phase response to DNA damage that is downstream from checkpoint activity. Normally, inhibition of DNA replication occurs when conditions are unfavorable to replication. This behavior appears less robust by flow cytometry analysis of bulk DNA replication in *mcl1*-1 cells than in control cells (Fig. 3A and C). Our previous work has shown that this diminished block to DNA replication does not result from a checkpoint defect, because *mcl1*-1 mutants are not defective in

where Cds1p was overexpressed (*mml1* GST-*cds1*) prior to 12 mM HU arrest. Gradients were fractionated into 22 0.5-ml fractions from the bottom (fraction 1) of the gradient. For reference, sedimentation of known standards with their relative molecular weights and sedimentation values are shown at the bottom of the α-GFP Western blots. (B) Western blot analysis of α-GFP immunoprecipitations from sucrose gradient fractions containing Mcl1-GFP show altered association with Pol1p in *hsk1*-1312 and *mml1* GST-*cds1* backgrounds but not *rad3*Δ and *cds1*Δ backgrounds. (C) GST-Pol1¹¹⁸⁻⁶³⁴-GSH-Sepharose coprecipitates Pol1p (top panel) and Mcl1GFP (middle panel) from *mcl1*-GFP, *hsk1*-1312, and *cds1*Δ but not from *mml1* GST-*cds1* whole-cell extracts. Immunodetection of GST molecules shows that this result is not due to the displacement of the GST-Pol1¹¹⁸⁻⁶³⁴ from the GSH-Sepharose by the coexpression of GST-Cds1p.

Cds1 kinase activation or cell cycle arrest in response to HU treatment (66).

The accumulation of replication intermediates in the *rad3Δ* mutant was extensive under mild replication stress, whereas we observed only a slight persistence of replication forks in *mcl1-1* mutants (Fig. 4). This result suggests that Mcl1 does not affect replication fork stability but affects some other replication function that is important for surviving replication arrest or DNA damage. One possibility, based on analogy with studies of Ctf4, is that polymerases are inappropriately allowed access to the DNA template in *mcl1* mutants, through unregulated Pol1 interaction with Pob3/Cdc68-like complexes. This would account for several properties of the *mcl1-1* cell line: the slight but apparent increase in DNA content associated with replication arrest in HU and MMS, the synergy between the *cds1Δ* and *mcl1-1* mutants in surviving HU, the strong mutator phenotype, and the synthetic lethality between the polymerase switch mutant *cdc24-M38* and *mcl1-1*. Alternatively, Mcl1p may be important for or affect DNA recombination. This could explain the poor recovery of replicating DNA, since a recent study with fission yeast suggests that recombination intermediates may be necessary for efficient origin activity (54) and the lethality between *rph51* and *rph54* with *mcl1-1* mutants.

Three pieces of evidence suggest that *mcl1-1*, *sepB3*, and *ctf4Δ* mutants have a high incidence of unresolved replication or recombination intermediates being carried into mitosis. First, these mutants have high rates of mitotic recombination and chromosomal rearrangement (32, 66). Second, these mutants have increased incidences of mitotic chromatin bridges, especially after HU treatment (20, 22, 66), which suggests that DNA cross-links between sister chromatids are not resolved prior to chromosome segregation. Third, these mutants appear to have a strong checkpoint-dependent delay to mitotic entry, and they depend on the RecQ helicase family for mitotic survival at permissive temperatures (24, 38, 66). Thus, the replication defects observed here for the *mcl1* mutants may result in increased mitotic recombination via break-induced replication following mitosis. This, in turn, would lead to dependence on Rad3, but not Cds1, since repair would need to occur prior to S phase in *mcl1* mutants.

One main unresolved question is the relationship between the increased recombination, replication defects, chromatin structure, and decreased sister chromatid cohesion seen in mutants of this family (58, 66). Our present hypothesis is that Mcl1 affects these multiple pathways through its role as Pol1p regulator, since Pol1 has distinct roles in each of these pathways. Alternatively, it is becoming increasingly evident that these pathways have intersecting roles that could be driven through a primary defect that gives rise to the multiple phenotypes, such that loss of chromatin structure precipitates the cohesion, replication, and recombination phenotypes.

ACKNOWLEDGMENTS

We thank G. Freyer, S. Sazar, T. S.-F. Wang, A. M. Carr, M. J. O'Connell, J. P. Javerzat, I. Hagan, A. Yamamoto, P. Russell, Susan Forsburg, and D. Q. Ding for yeast strains and reagents.

This work was supported by National Institutes of Health grant GM-33787 to J.R.M., who is a Research Professor of the American Cancer Society.

REFERENCES

- Ahmed, S., S. Saini, S. Arora, and J. Singh. 2001. Chromodomain protein Swi6-mediated role of DNA polymerase alpha in establishment of silencing in fission yeast. *J. Biol. Chem.* **276**:47814–47821.
- Bailis, J. M., P. Bernard, R. Antonelli, R. C. Allshire, and S. L. Forsburg. 2003. Hsk1-Dfp1 is required for heterochromatin-mediated cohesion at centromeres. *Nat. Cell Biol.* **5**:1111–1116.
- Bernard, P., J.-F. Maure, J. F. Partridge, S. Genier, J.-P. Javerzat, and R. C. Allshire. 2001. Requirement of heterochromatin for cohesion at centromeres. *Science* **294**:2539–2542.
- Birkenbihl, R. P., and S. Subramani. 1992. Cloning and characterization of *rad21* an essential gene of *Schizosaccharomyces pombe* involved in DNA double-strand-break repair. *Nucleic Acids Res.* **20**:6605–6611.
- Biswas, S. B., S. M. Khopde, F. X. Zhu, and E. E. Biswas. 2003. Subunit interactions in the assembly of *Saccharomyces cerevisiae* DNA polymerase α . *Nucleic Acids Res.* **31**:2056–2065.
- Boddy, M. N., B. Furnari, O. Mondesert, and P. Russell. 1998. Replication checkpoint enforced by kinases Cds1 and Chk1. *Science* **280**:909–912.
- Brown, G. W., and T. J. Kelly. 1998. Purification of Hsk1, a minichromosome maintenance protein kinase from fission yeast. *J. Biol. Chem.* **273**:22083–22090.
- Craven, R. A., D. J. Griffiths, K. S. Sheldrick, R. E. Randall, I. M. Hagan, and A. M. Carr. 1998. Vectors for the expression of tagged proteins in *Schizosaccharomyces pombe*. *Gene* **221**:59–68.
- Dahlen, M., T. Olsson, G. Kanter-Smoler, A. Ramne, and P. Sunnerhagen. 1998. Regulation of telomere length by checkpoint genes in *Schizosaccharomyces pombe*. *Mol. Biol. Cell* **9**:611–621.
- Dehde, S., O. Schub, G. Rohaly, H.-P. Nasheuer, W. Bohn, J. Chemnitz, W. Deppert, and I. Dornreiter. 2001. Two immunologically distinct human DNA polymerase α -primase subpopulations are involved in cellular DNA replication. *Mol. Cell. Biol.* **21**:2581–2593.
- Diede, S. J., and D. E. Gottschling. 1999. Telomerase-mediated telomere addition in vivo requires DNA primase and DNA polymerases alpha and delta. *Cell* **99**:723–733.
- Ding, D. Q., Y. Tomita, A. Yamamoto, Y. Chikashige, T. Haraguchi, and Y. Hiraoka. 2000. Large-scale screening of intracellular protein localization in living fission yeast cells by the use of a GFP-fusion genomic DNA library. *Genes Cells* **5**:169–190.
- Dohrmann, P. R., G. Oshiro, M. Tecklenburg, and R. A. Sclafani. 1999. RAD53 regulates DBF4 independently of checkpoint function in *Saccharomyces cerevisiae*. *Genetics* **151**:965–977.
- Duncker, B. P., K. Shimada, M. Tsai-Pflugfelder, P. Pasero, and S. M. Gasser. 2002. An N-terminal domain of Dbp4p mediates interaction with both origin recognition complex (ORC) and Rad53p and can deregulate late origin firing. *Proc. Natl. Acad. Sci. USA* **99**:16087–16092.
- D'Urso, G., B. Grallert, and P. Nurse. 1995. DNA polymerase alpha, a component of the replication initiation complex, is essential for the checkpoint coupling S phase to mitosis in fission yeast. *J. Cell Sci.* **108**:3109–3118.
- Evan, G. I., G. K. Lewis, G. Ramsay, and J. M. Bishop. 1985. Isolation of monoclonal antibodies specific for human *c-myc* proto-oncogene product. *Mol. Cell. Biol.* **5**:3610–3616.
- Fan, X., and C. M. Price. 1997. Coordinate regulation of G- and C strand length during new telomere synthesis. *Mol. Biol. Cell* **8**:2145–2155.
- Ferrari, M., G. Lucchini, P. Plevani, and M. Foiani. 1996. Phosphorylation of the DNA polymerase alpha-primase B subunit is dependent on its association with the p180 polypeptide. *J. Biol. Chem.* **271**:8661–8666.
- Formosa, T., P. Eriksson, J. Wittmeyer, J. Ginn, Y. Yu, and D. J. Stillman. 2001. Spt16-Pob3 and the HMG protein Nhp6 combine to form the nucleosome-binding factor SPN. *EMBO J.* **20**:3506–3517.
- Formosa, T., and T. Nittis. 1999. Dna2 mutants reveal interactions with DNA polymerase alpha and Ctf4, a Pol alpha accessory factor, and show that full Dna2 helicase activity is not essential for growth. *Genetics* **151**:1459–1470.
- Hanna, J. S., E. S. Kroll, V. Lundblad, and F. A. Spencer. 2001. *Saccharomyces cerevisiae* CTF18 and CTF4 are required for sister chromatid cohesion. *Mol. Cell. Biol.* **21**:3144–3158.
- Harris, S. D., and J. E. Hamer. 1995. *sepB*: an *Aspergillus nidulans* gene involved in chromosome segregation and the initiation of cytokinesis. *EMBO J.* **14**:5244–5257.
- Hartwell, L. H., and T. A. Weinert. 1989. Checkpoints: controls that ensure the order of cell cycle events. *Science* **246**:629–634.
- Hofmann, A. F., and S. D. Harris. 2000. The *Aspergillus nidulans* *uvsB* gene encodes an ATM-related kinase required for multiple facets of the DNA damage response. *Genetics* **154**:1577–1586.
- Hollingsworth, R. E., Jr., R. M. Ostroff, M. B. Klein, L. A. Niswander, and R. A. Sclafani. 1992. Molecular genetic studies of the Cdc7 protein kinase and induced mutagenesis in yeast. *Genetics* **132**:53–62.
- Jiang, W., and T. Hunter. 1997. Identification and characterization of a human protein kinase related to budding yeast Cdc7p. *Proc. Natl. Acad. Sci. USA* **94**:14320–14325.
- Kearsey, S. E., S. Montgomery, K. Labib, and K. Lindner. 2000. Chromatin

- binding of the fission yeast replication factor mcm4 occurs during anaphase and requires ORC and cdc18. *EMBO J.* **19**:1681–1690.
28. Kelly, T. J., and G. W. Brown. 2000. Regulation of chromosome replication. *Annu. Rev. Biochem.* **69**:829–880.
 29. Kihara, M., W. Nakai, S. Asano, A. Suzuki, K. Kitada, Y. Kawasaki, L. H. Johnston, and A. Sugino. 2000. Characterization of the yeast Cdc7p/Dbf4p complex purified from insect cells. Its protein kinase activity is regulated by Rad53p. *J. Biol. Chem.* **275**:35051–35062.
 30. Kim, S. M., and J. A. Huberman. 2001. Regulation of replication timing in fission yeast. *EMBO J.* **20**:6115–6126.
 31. Kohler, A., M. S. Schmidt-Zachmann, and W. W. Franke. 1997. AND-1, a natural chimeric DNA-binding protein, combines an HMG-box with regulatory WD-repeats. *J. Cell Sci.* **110**:1051–1062.
 32. Kouprina, N., E. Kroll, V. Bannikov, V. Bliskovsky, R. Gizatullin, A. Kirillov, B. Shestopalov, V. Zakharyev, P. Hieter, F. Spencer, et al. 1992. CTF4 (CHL15) mutants exhibit defective DNA metabolism in the yeast *Saccharomyces cerevisiae*. *Mol. Cell. Biol.* **12**:5736–5747.
 33. Lane, E. H. A. D. 1998. Using antibodies: a laboratory manual, 2nd ed. Cold Spring Harbor Laboratory Press, Cold Spring Harbor, N.Y.
 34. Lei, M., Y. Kawasaki, M. R. Young, M. Kihara, A. Sugino, and B. K. Tye. 1997. Mcm2 is a target of regulation by Cdc7-Dbf4 during the initiation of DNA synthesis. *Genes Dev.* **11**:3365–3374.
 35. Marchetti, M. A., S. Kumar, E. Hartsuiker, M. Maftahi, A. M. Carr, G. A. Freyer, W. C. Burhans, and J. A. Huberman. 2002. A single unbranched S-phase DNA damage and replication fork blockage checkpoint pathway. *Proc. Natl. Acad. Sci. USA* **99**:7472–7477.
 36. Martin, A. A., I. Dionne, R. J. Wellinger, and C. Holm. 2000. The function of DNA polymerase α at telomeric G tails is important for telomere homeostasis. *Mol. Cell. Biol.* **20**:786–796.
 37. Michael, W. M., R. Ott, E. Fanning, and J. Newport. 2000. Activation of the DNA replication checkpoint through RNA synthesis by primase. *Science* **289**:2133–2137.
 38. Miles, J., and T. Formosa. 1992. Evidence that POB1, a *Saccharomyces cerevisiae* protein that binds to DNA polymerase alpha, acts in DNA metabolism in vivo. *Mol. Cell. Biol.* **12**:5724–5735.
 39. Mizuno, T., K. Yamagishi, H. Miyazawa, and F. Hanaoka. 1999. Molecular architecture of the mouse DNA polymerase α -primase complex. *Mol. Cell. Biol.* **19**:7886–7896.
 40. Moreno, S., A. Klar, and P. Nurse. 1991. Molecular genetic analysis of fission yeast *Schizosaccharomyces pombe*. *Methods Enzymol.* **194**:795–823.
 41. Nakayama, J., R. C. Allshire, A. J. Klar, and S. I. Grewal. 2001. A role for DNA polymerase alpha in epigenetic control of transcriptional silencing in fission yeast. *EMBO J.* **20**:2857–2866.
 42. Okuhara, K., K. Ohta, H. Seo, M. Shioda, T. Yamada, Y. Tanaka, N. Dohmae, Y. Seyama, T. Shibata, and H. Murofushi. 1999. A DNA unwinding factor involved in DNA replication in cell-free extracts of *Xenopus* eggs. *Curr. Biol.* **9**:341–350.
 43. Oshiro, G., J. C. Owens, Y. Shellman, R. A. Sclafani, and J. J. Li. 1999. Cell cycle control of Cdc7p kinase activity through regulation of Dbf4p stability. *Mol. Cell. Biol.* **19**:4888–4896.
 44. Ostroff, R. M., and R. A. Sclafani. 1995. Cell cycle regulation of induced mutagenesis in yeast. *Mutat. Res.* **329**:143–152.
 45. Paciotti, V., M. Clerici, M. Scotti, G. Lucchini, and M. P. Longhese. 2001. Characterization of *mec1* kinase-deficient mutants and of new hypomorphic *mec1* alleles impairing subsets of the DNA damage response pathway. *Mol. Cell. Biol.* **21**:3913–3925.
 46. Park, H., R. Davis, and T. S. Wang. 1995. Studies of *Schizosaccharomyces pombe* DNA polymerase alpha at different stages of the cell cycle. *Nucleic Acids Res.* **23**:4337–4344.
 47. Park, H., S. Francesconi, and T. S. Wang. 1993. Cell cycle expression of two replicative DNA polymerases alpha and delta from *Schizosaccharomyces pombe*. *Mol. Biol. Cell* **4**:145–157.
 48. Paulovich, A. G., R. U. Margulies, B. M. Garvik, and L. H. Hartwell. 1997. RAD9, RAD17, and RAD24 are required for S phase regulation in *Saccharomyces cerevisiae* in response to DNA damage. *Genetics* **145**:45–62.
 49. Postow, L., N. J. Crisona, B. J. Peter, C. D. Hardy, and N. R. Cozzarelli. 2001. Topological challenges to DNA replication: conformations at the fork. *Proc. Natl. Acad. Sci. USA* **98**:8219–8226.
 50. Postow, L., C. Ullsperger, R. W. Keller, C. Bustamante, A. V. Vologodskii, and N. R. Cozzarelli. 2001. Positive torsional strain causes the formation of a four-way junction at replication forks. *J. Biol. Chem.* **276**:2790–2796.
 51. Qi, H., and V. A. Zakian. 2000. The *Saccharomyces* telomere-binding protein Cdc13p interacts with both the catalytic subunit of DNA polymerase alpha and the telomerase-associated Est1 protein. *Genes Dev.* **14**:1777–1788.
 52. Ray, S., Z. Karamysheva, L. Wang, D. E. Shippen, and C. M. Price. 2002. Interactions between telomerase and primase physically link the telomere and chromosome replication machinery. *Mol. Cell. Biol.* **22**:5859–5868.
 53. Santocanale, C., and J. F. Diffley. 1998. A Mec1- and Rad53-dependent checkpoint controls late-firing origins of DNA replication. *Nature* **395**:615–618.
 54. Segurado, M., M. F. Gomez, and F. Antequera. 2002. Increased recombination intermediates and homologous integration hot spots at DNA replication origins. *Mol. Cell. Biol.* **22**:907–916.
 55. Snaith, H. A., G. W. Brown, and S. L. Forsburg. 2000. *Schizosaccharomyces pombe* Hsk1p is a potential Cds1p target required for genome integrity. *Mol. Cell. Biol.* **20**:7922–7932.
 56. Sogo, J. M., M. Lopes, and M. Foiani. 2002. Fork reversal and ssDNA accumulation at stalled replication forks owing to checkpoint defects. *Science* **297**:599–602.
 57. Stillman, B. 1989. Initiation of eukaryotic DNA replication in vitro. *Annu. Rev. Cell Biol.* **5**:197–245.
 58. Suter, B., A. Tong, M. Chang, L. Yu, G. W. Brown, C. Boone, and J. Rine. 2004. The origin recognition complex links replication, sister chromatid cohesion and transcriptional silencing in *Saccharomyces cerevisiae*. *Genetics* **167**:579–591.
 59. Takeda, T., K. Ogino, E. Matsui, M. K. Cho, H. Kumagai, T. Miyake, K. Arai, and H. Masai. 1999. A fission yeast gene, *him1⁺dpl1⁺*, encoding a regulatory subunit for Hsk1 kinase, plays essential roles in S-phase initiation as well as in S-phase checkpoint control and recovery from DNA damage. *Mol. Cell. Biol.* **19**:5535–5547.
 60. Takeda, T., K. Ogino, K. Tatebayashi, H. Ikeda, K. Arai, and H. Masai. 2001. Regulation of initiation of S phase, replication checkpoint signaling, and maintenance of mitotic chromosome structures during S phase by Hsk1 kinase in the fission yeast. *Mol. Biol. Cell* **12**:1257–1274.
 61. Tercero, J. A., and J. F. Diffley. 2001. Regulation of DNA replication fork progression through damaged DNA by the Mec1/Rad53 checkpoint. *Nature* **412**:553–557.
 62. Tercero, J. A., M. P. Longhese, and J. F. Diffley. 2003. A central role for DNA replication forks in checkpoint activation and response. *Mol. Cell* **11**:1323–1336.
 63. Waga, S., and B. Stillman. 1998. The DNA replication fork in eukaryotic cells. *Annu. Rev. Biochem.* **67**:721–751.
 64. Warren, C. D., D. M. Eckley, M. S. Lee, J. S. Hanna, A. Hughes, B. Peyser, C. Jie, R. Irizarry, and F. A. Spencer. 2004. S-phase checkpoint genes safeguard high fidelity sister chromatid cohesion. *Mol. Biol. Cell* **15**:1724–1735.
 65. Weinreich, M., and B. Stillman. 1999. Cdc7p-Dbf4p kinase binds to chromatin during S phase and is regulated by both the APC and the RAD53 checkpoint pathway. *EMBO J.* **18**:5334–5346.
 66. Williams, D. R., and J. R. McIntosh. 2002. *mcl1⁺*, the *Schizosaccharomyces pombe* homologue of CTF4, is important for chromosome replication, cohesion, and segregation. *Eukaryot. Cell* **1**:758–773.
 67. Wittmeyer, J., and T. Formosa. 1997. The *Saccharomyces cerevisiae* DNA polymerase α catalytic subunit interacts with Cdc68/Spt16 and with Pob3, a protein similar to an HMG1-like protein. *Mol. Cell. Biol.* **17**:4178–4190.
 68. You, Z., L. Kong, and J. Newport. 2002. The role of single-stranded DNA and polymerase alpha in establishing the ATR, Hus1 DNA replication checkpoint. *J. Biol. Chem.* **277**:27088–27093.